Alfvén multistability: Transient and intermittent dynamics induced by noise

Erico L. Rempel[a)]
Institute of Aeronautical Technology (ITA) and World Institute for Space Environment Research (WISER), CTA/ITA/IEFM, São José dos Campos-SP, 12228-900, Brazil

Wanderson M. Santana and Abraham C.-L. Chian
National Institute for Space Research (INPE) and World Institute for Space Environment Research (WISER), P.O. Box 515, São José dos Campos-SP, 12227-010, Brazil

The effects of noise in the dynamics of Alfvén waves described by the derivative nonlinear Schrödinger equation are investigated. In a complex region of the parameter space, where multistability is observed, an external stochastic source can effectively destroy attractors present in the noise-free system, as well as induce chaotic transients and extrinsic intermittency. In the intermittent regime, the Alfvén wave exhibits random qualitative changes in its behavior as a result of a competition between three attractors and a chaotic saddle embedded in the fractal basin boundary. © *2006 American Institute of Physics*. [DOI: 10.1063/1.2186527]

I. INTRODUCTION

Chaos theory provides powerful tools for the study of theoretical and experimental plasma systems. In laboratory plasmas, Cheung and Wong[1] reported the experimental observation of chaotic behavior in a pulsed plasma discharge, with a calculation of the Feigenbaum constant for a period-doubling route to chaos. The period-doubling route to chaos was also studied by Greiner *et al.*[2] by comparing results from a filament cathode discharge with particle-in-cell simulations. Sheridam[3] conducted the experimental characterization of chaotic dynamics in a complex (dusty) plasma of three particles, with the detection of an attractor with fractal dimension and a positive Lyapunov exponent.

Most theoretical works on chaotic dynamics in plasmas are based on noise-free numerical simulations. In this paper we are concerned with the analysis of Alfvén waves in multistable systems in the presence of noise. In dynamical systems, multistability refers to the simultaneous presence of more than one attractor for a given value of the control parameter. Attractors are the asymptotic states in dissipative systems, and multistability can be an obstacle for prediction, since the asymptotic state may depend crucially on the initial condition. Thus, knowledge about the attractors and their respective basins of attraction is essential for understanding the dynamics of multistable systems.

There is a number of theoretical works on multistability, both in mathematical models and real plasma experiments. A mathematical model for drift waves studied in Refs. 4 and 5 in relation to the transition to spatiotemporal chaos was shown to exhibit hysteresis loops, which correspond to multistability. Chian *et al.*[6] characterized the origin, evolution, and destruction of attractors in a complex region of the parameter space of the derivative nonlinear Schrödinger equation, where up to four different attractors coexist. Hahn and Pae[7] reported the observation of competing multistability in plasma diode systems by using one-dimensional particle-in-cell simulations. Intrinsic numerical noise is found to be responsible for causing attractor hopping, resulting in a complicated time series.[7,8] Coninck *et al.*[9] investigated the coexistence of a large number of periodic attractors in a system of four waves interacting by means of nonlinear coupling between two wave triplets. Multistability has also been reported in experimental plasma systems. Chern and I[10] performed an experimental study of bifurcations leading to hysteresis in a weakly ionized cylindrical rf magnetoplasma system. Sun *et al.*[11] investigated multistability and crisis-induced intermittency in experiments with a plasma discharge system.

In this paper we focus on the role of noise in the generation of transient and intermittent behavior in Alfvén waves modeled by the derivative nonlinear Schrödinger (DNLS) equation, where multistability is observed. Alfvén waves are ubiquitous in space and laboratory plasmas, and are important to plasma heating and particle acceleration in the solar corona,[12,13] auroral,[14] as well as tokamaks and other laboratory plasmas.[15,16] We show that noise can couple attracting and nonattracting chaotic sets (chaotic saddles) in the phase space of the DNLS equation, resulting in complex intermittent dynamics of an Alfvén magnetic field. In Sec. II we describe the driven-dissipative DNLS equation and its stationary solutions. In Sec. III we present a region of the parameter space of the DNLS equation with multistability and discuss the origin and destruction of attractors and their basins of attraction. By adding noise to the DNLS equation, we show in Sec. IV that it is possible to generate extrinsic transient behavior that is similar to the dynamics after an attractor-destruction crisis (boundary crisis) in noise-free systems.[6,17,18] In Sec. V we show that noise can induce intermittent behavior similar to the intermittency observed after an attractor merging crisis.[18–20] The conclusions are given in Sec. VI.

[a)]Corresponding author. Electronic mail: rempel@ita.br

13, 032308-1

II. THE DERIVATIVE NONLINEAR SCHRÖDINGER EQUATION

The nonlinear spatiotemporal evolution of Alfvén waves can be modeled by the driven-dissipative derivative nonlinear Schrödinger equation (DNLS),[21]

$$\partial_t b + \alpha \partial_x(|b|^2 b) - i(\mu + i\eta)\partial_x^2 b = S(b,x,t), \tag{1}$$

where the wave is propagating along an ambient magnetic field B_0 in the x direction, $b=b_y+ib_z$ is the complex transverse wave magnetic field normalized to the constant ambient magnetic field, η is the dissipative scale length, time t is normalized to the inverse of the ion cyclotron frequency $\omega_{ci}=eB_0/m_i$, space x is normalized to c_A/ω_{ci}, $c_A =B_0/(\mu_0\rho_0)^{1/2}$ is the Alfvén velocity, $\alpha=1/[4(1-\beta)]$, $\beta =c_S^2/c_A^2$, $c_S=(\gamma P_0/\rho_0)^{1/2}$ is the acoustic velocity, and μ is the dispersive parameter. The external forcing $S(b,x,t) =A\exp(ik\phi)$ is a monochromatic left-hand circularly polarized wave with a wave phase $\phi=x-Vt$, where V is a constant wave velocity, A is the driver amplitude, and k is the driver wave number.

By seeking stationary solutions with $b=b(\phi)$, and setting $\partial_t b=0$, the first integral of Eq. (1) reduces to a low-dimensional system of coupled ordinary differential equations,

$$\dot{b}_y - \nu\dot{b}_z = \partial H/\partial b_z + a\cos\theta, \tag{2}$$

$$\dot{b}_z + \nu\dot{b}_y = -\partial H/\partial b_y + a\sin\theta, \tag{3}$$

$$\dot{\theta} = \Omega, \tag{4}$$

where $H=(\mathbf{b}^2-1)^2/4-(\lambda/2)(\mathbf{b}-\hat{\mathbf{y}})^2$, the overdot denotes the derivative with respect to the phase variable $\tau=\alpha b_0^2\phi/\mu$, $\nu =\eta/\mu$ is the normalized dissipation parameter, $b\rightarrow b/b_0$ (where b_0 is an integration constant), $\mathbf{b}=(b_y,b_z)$, $\theta=\Omega\phi$, $\Omega =\mu k/(\alpha b_0^2)$, $a=A/(\alpha b_0^2 k)$, $\lambda=-1+V/(\alpha b_0^2)$. We assume $\beta <1$, hence $\alpha>0$.

In order to study the nonlinear dynamics of the system (2)–(4), we treat the phase variable τ as a "time" variable and define the following Poincaré map:

$$P:[b_y(\tau),b_z(\tau)] \rightarrow [b_y(\tau+T),b_z(\tau+T)], \tag{5}$$

$$\tau \rightarrow \tau+T, \tag{6}$$

where $T=2\pi/\Omega$ is the driver period and $b(\tau)$ represents the value of b at time τ. Thus, one iteration of the Poincaré map, $P[b(\tau)]$, corresponds to integrating Eqs. (2)–(4) from time τ to time $\tau+T$. This type of projection defined in fixed time intervals is called stroboscopic projection, or the time-T map. In the following sections we use $\tau=0$ for the initial phase and generate trajectories in the plane (b_y,b_z) by plotting one *Poincaré point* at each value of $\tau+nT$, $n=1,2,\dots$.

III. MULTISTABILITY IN THE DNLS EQUATION

The nonlinear system described by Eqs. (2)–(4) can display a wealth of dynamical phenomena depending on the choice of control parameters and initial conditions. Chian *et al.*[6] identified a range of ν for which there is a coexistence of
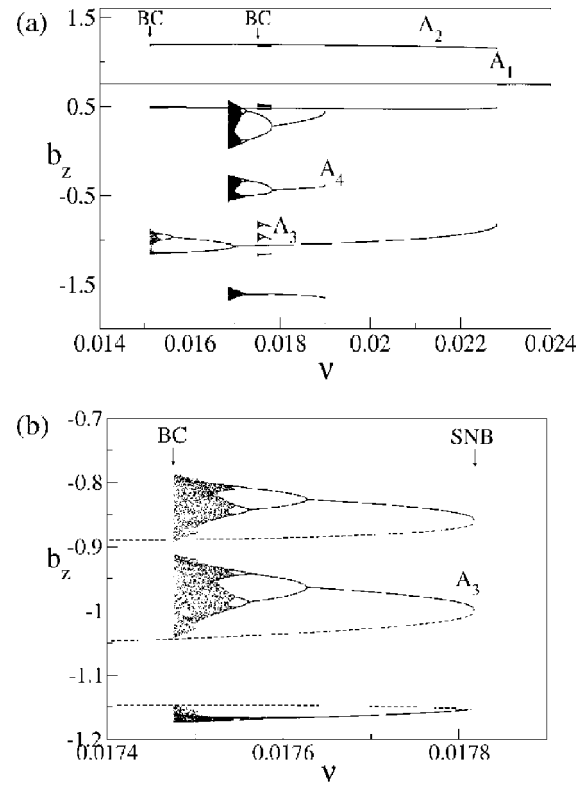

FIG. 1. (a) Bifurcation diagram, b_z vs. ν, for Eqs. (2)–(4) showing the evolution of four distinct attractors (A_1, A_2, A_3, and A_4); (b) enlargement of a portion of (a) showing attractor (A_3). BC denotes the boundary crisis and the dashed lines represent the unstable periodic orbit responsible for the crisis.

attractors in the DNLS equation. Four different attractors are plotted in the bifurcation diagram of Fig. 1(a), where we set $a=0.1$, $\Omega=-1$ $\lambda=1/4$, $\mu=1/2$ and plot the Poincaré points of b_z vs.. ν. Attractor A_1 corresponds to a stable periodic Alfvén wave of period 1 in the Poincaré map. Attractor A_2 is born in a *saddle-node bifurcation* at $\nu\sim0.0227$ as a period-3 periodic wave and suffers a *period doubling cascade* route to chaos as ν is decreased. The chaotic attractor A_2 disappears abruptly at $\nu\sim0.015\,14$ in a global bifurcation known as a *boundary crisis* (BC).[17] Attractor A_3 suffers a similar sequence of bifurcations, starting as a period-9 stable periodic wave at a saddle-node bifurcation at $\nu\sim0.017\,816\,2$ and ending in a boundary crisis at $\nu\sim0.017\,477\,1$. Attractor A_4 is born as a period-3 stable wave at $\nu\sim0.019$ and ends in a boundary crisis at $\nu\sim0.016\,853$. There is a fifth attractor, not shown in Fig. 1(a), which exists in a tiny region of the bifurcation diagram around $\nu\sim0.017\,145$. Thus, the small range of ν between 0.014 and 0.024 encloses at least five different attracting sets.

The mechanisms of creation and destruction of the attractors of Fig. 1(a) are illustrated in Fig. 1(b), which is an enlargement of Fig. 1(a) showing three of the nine branches of the bifurcation diagram of attractor A_3. The dashed lines denote the Poincaré points of a period-9 unstable periodic wave created simultaneously with the stable periodic wave at the saddle-node bifurcation at $\nu\sim0.017\,816\,2$, indicated as SNB. As ν is decreased, the unstable wave approaches the chaotic attractor evolved from the cascade of period dou-
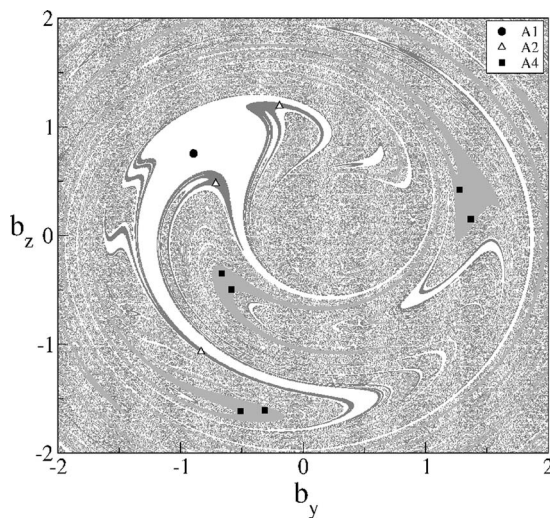
FIG. 2. Periodic attractors A_1 (circle), A_2 (triangles), and A_4 (squares) and their basins of attraction in white (A_1), dark gray (A_2), and light gray (A_4), at $\nu=0.017\,46$.

FIG. 3. Chaotic saddle on the boundary separating the basins of attraction at $\nu=0.017\,46$.

bling bifurcations of A_3, and at $\nu \sim 0.017\,477\,1$ the two sets collide head on, causing the boundary crisis (BC), which is responsible for the destruction of A_3. This crisis was studied in detail in Chian et al.[6]

We now focus on the dynamics at $\nu=0.017\,46$, where three periodic attractors coexist. In the Poincaré map a period-n periodic wave turns into a set of n points. Figure 2 depicts the Poincaré map of attractors A_1 (circle, period 1), A_2 (triangles, period 3) and A_4 (squares, period 6), and their *basins of attraction*. The basin of attraction is the set of initial conditions in the (b_y, b_z) phase plane that converge to a given attractor. Hence, the white region in Fig. 2 is the basin of A_1, dark gray represents the basin of A_2 and light gray the basin of A_4. The basin boundaries display a complex structure in most of the phase plane, where the three basins seem to mingle. This complex structure is scale invariant, a typical property of fractal sets. Embedded in the basin boundary, we numerically found a nonattracting chaotic set known as a *chaotic saddle*. Chaotic saddles are ubiquitous in nonlinear systems and are chiefly responsible for transient chaotic motion.[17,22,23] The chaotic saddle in Fig. 3 was found with the sprinkler method,[22] and its role in attractor hopping and Alfvén intermittency is discussed in the following sections.

IV. NOISE-INDUCED TRANSIENTS AND ATTRACTOR DESTRUCTION

We introduce an external stochastic source in the Alfvén system by adding noise terms $g_y(t)$ and $g_z(t)$ to Eqs. (2) and (3), respectively, where $g_y(t)$ and $g_z(t)$ are provided by a random numbers generator with a Gaussian distribution with zero mean and standard deviation σ. The effect of noise in the bifurcation diagram for attractor A_4 is seen in Fig. 4. Figure 4(a) displays the noise-free diagram ($\sigma=0$), and Fig. 4(b) shows the same diagram for $\sigma=0.0025$, where the cascade of period doubling bifurcations is obscured by noise and the transition to chaos cannot be precisely determined.
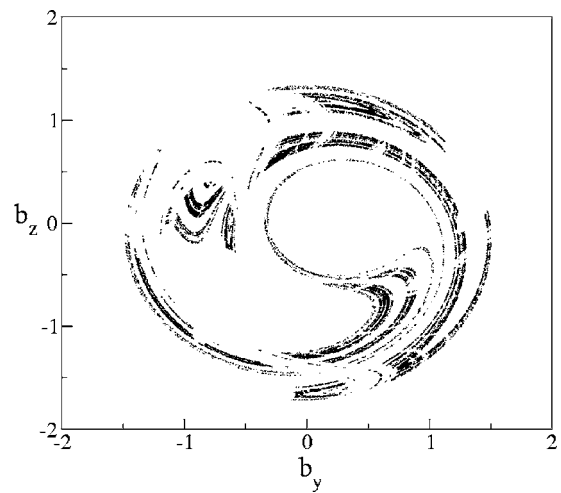
Figure 4(b) is much more realistic than Fig. 4(a), since noise is always present in nature. Figure 4(b) is similar to real bifurcation diagrams found in plasma experiments.[1,2]

Figure 5 illustrates the effect of noise on the time series of b_z for period-6 attractor A_4 at $\nu=0.017\,46$. Figure 5(a) displays the noise-free ($\sigma=0$) time-2π time series in terms of

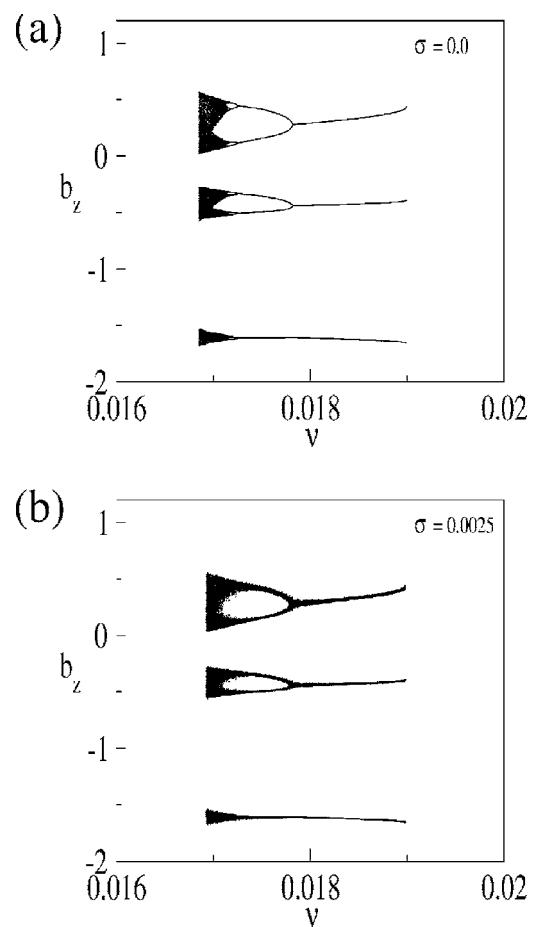FIG. 4. (a) Noise-free ($\sigma=0$) bifurcation diagram for attractor A_4; (b) noisy bifurcation diagram for $\sigma=0.0025$.
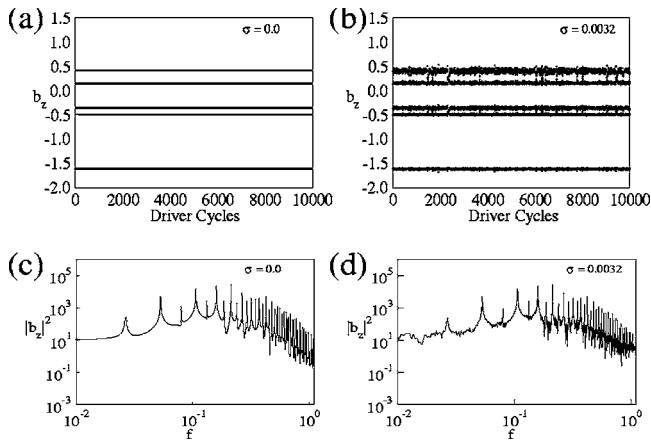
FIG. 5. Time-2π time series of b_z in terms of the driver cycles for period-6 attractor A_4 at $\nu=0.017\,46$ (a) without noise; (b) with Gaussian noise using a zero mean and a standard deviation of $\sigma=0.0032$; (c) and (d) the corresponding power spectra.

the driver cycles and Fig. 5(b) show the same time series for $\sigma=0.0032$. The corresponding power spectra are shown in Figs. 5(c) and 5(d), respectively. The spectrum in Fig. 5(d) contains the same spikes of Fig. 5(c), indicating the predominant frequencies of the solution. In addition, the spectrum of the noisy periodic wave shown in Fig. 5(d) has a continuous, broadband nature, typical of chaotic Alfvén waves.[24] It is also a feature found in power density spectra of turbulent Alfvénic fluctuations observed in the solar wind.[25,26]

The noisy basins of attraction for A_1, A_2, and A_4 are plotted in Fig. 6, together with the (b_y, b_z) Poincaré points of A_4. Note that in the presence of noise A_4 resembles a chaotic attractor, stretching along directions for which attraction is weakest, as previously noted by Gwinn and Westervelt.[27,28] The bigger the noise, the more stretched is the attractor, so that initial conditions in the light gray region of Fig. 6 will produce Alfvén waves that are confined to this basin as long as A_4 does not touch its basin boundary. If the noise level is strong enough to stretch A_4 beyond its basin boundary, the
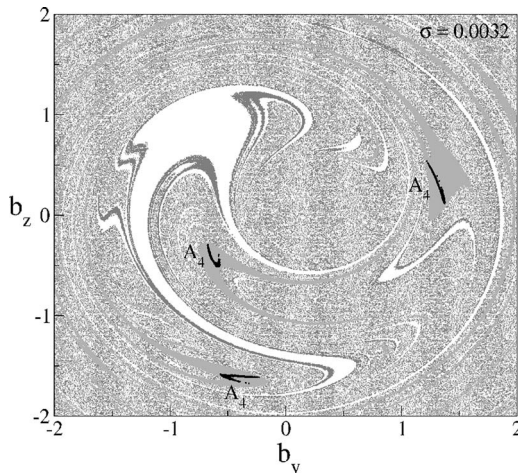

FIG. 6. Basins of attraction and attractor A_4 at $\nu=0.017\,46$ in the presence of noise ($\sigma=0.0032$). The enlarged attractor A_4 does not touch its basin boundary.
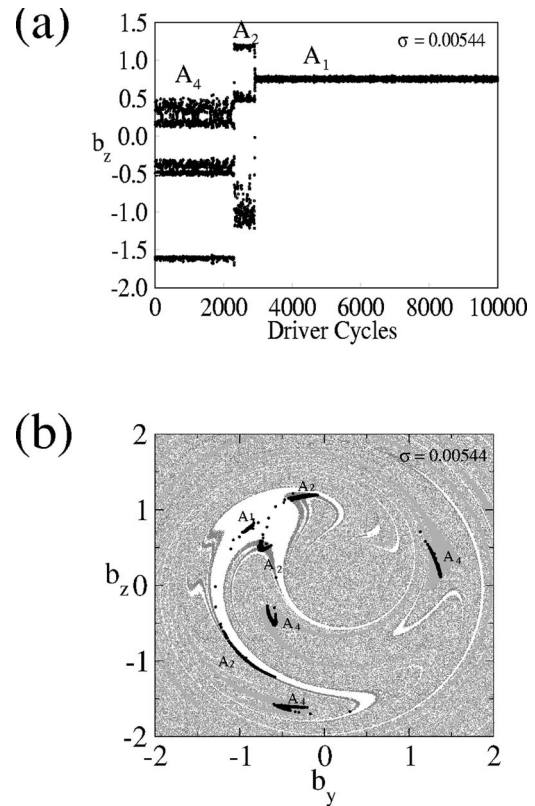

FIG. 7. (a) Noise induced transient for $\sigma=0.00544$ at $\nu=0.017\,46$, showing attractor hopping from A_4 to A_2, then to A_1; (b) Poincaré map of the time series in (a) with basins of attraction.

Alfvén wave "escapes" from the gray region, wanders for a short time in the complex boundary region before settling to a different attractor, when an *attractor hopping* occurs.[29,30] Figure 7(a) shows attractor hopping from A_4 to A_2 then to A_1, when noise is set to $\sigma=0.005\,44$. In Fig. 7(b) the Poincaré map corresponding to the time series in Fig. 7(a) is plotted over the noisy basins of attraction. Since A_1 has a wide basin, this noise level is not strong enough to "kick" the wave out of the white basin, and the noisy A_1 attractor is the asymptotic state of each initial condition in Fig. 7(b). Thus, the hopping between attractors A_4 and A_2 constitutes a noise-induced, or extrinsic, transient dynamics.

The generation of noise-induced transients is akin to an attractor destruction due to a boundary crisis. Recall from Fig. 1(a) that attractor A_2 is destroyed in a boundary crisis at $\nu=\nu_{BC}\sim0.015\,14$. Thus, for $\nu<0.015\,14$ initial conditions in the region of the phase plane previously occupied by A_2 will eventually leave this region, moving to another attractor. It has been shown that the average transient time before the wave leaves the region previously occupied by the destroyed attractor depends on the value of the control parameter in relation to the critical crisis value.[18] Hence, for ν very close to ν_{BC} the magnetic field of Alfvén waves will oscillate for a long transient time in the region of A_2 before leaving it. As ν is decreased away from ν_{BC}, the average transient time decreases proportionally. This effect is illustrated in Figs. 8(a)–8(c) for three different values of ν just before [$\nu=0.015\,14$, Fig. 8(a)], right after [$\nu=0.015\,13$, Fig. 8(b)], and farther away [$\nu=0.015\,12$, Fig. 8(a)] from crisis. By
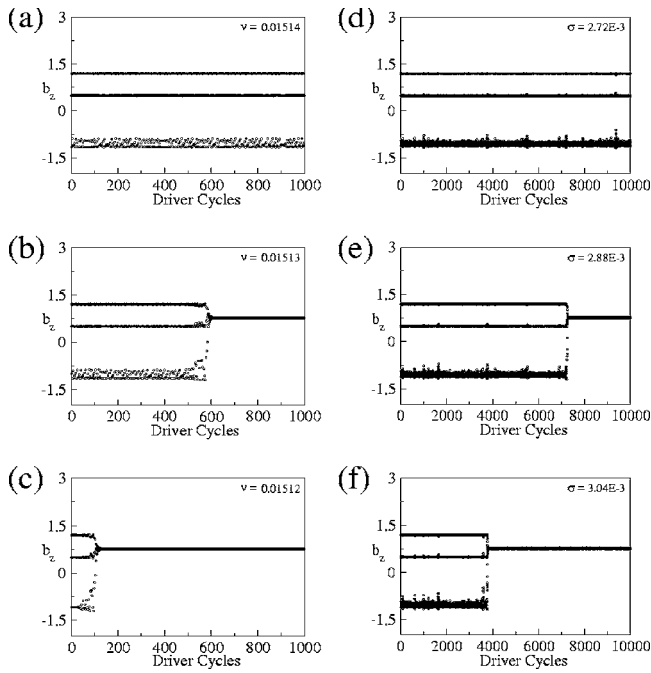
FIG. 8. Intrinsic (a)–(c) and extrinsic (d)–(f) chaotic transients. (a) Chaotic time series of A_2 just before a boundary crisis at $\nu=0.015\ 14$; (b) chaotic transient right after the boundary crisis of A_2 at $\nu=0.015\ 13$; (c) reduction of the transient time farther away from crisis at $\nu=0.015\ 12$; (d) noise induced chaos in A_2 at $\nu=0.017\ 46$ with $\sigma=0.002\ 72$; (e) chaotic transient at $\nu=0.017\ 46$ due to increased noise ($\sigma=0.002\ 88$); (f) reduction of the transient at $\nu=0.017\ 46$ following increase in noise ($\sigma=0.003\ 04$).
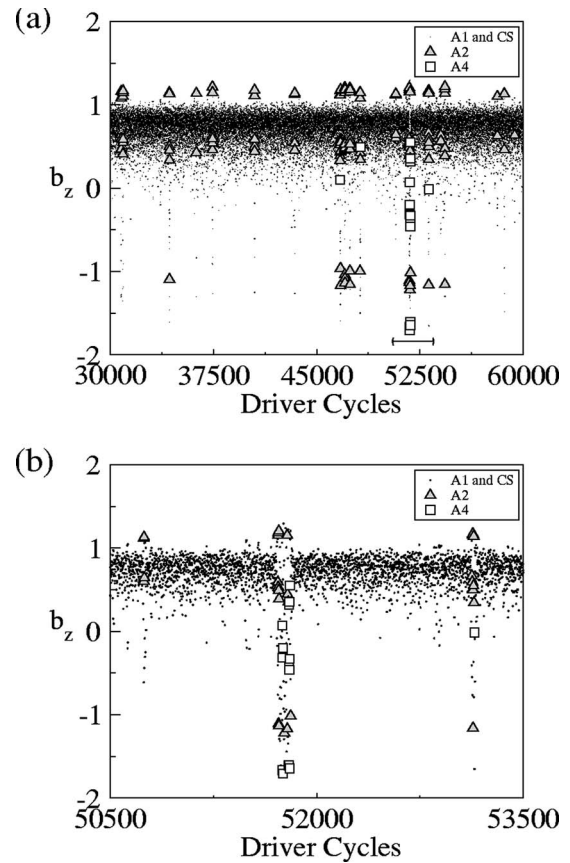

FIG. 9. (a) Noise induced intermittency at $\nu=0.017\ 46$, for $\sigma=0.064$. Triangles are plotted whenever the orbit is in the vicinity of attractor A_2 and squares refer to the vicinity of A_4. Circles represent points in the vicinity of A_1 or the surrounding chaotic saddle (CS). (b) Enlargement of an interval in (a).

adding noise to the system we are able to see a similar effect without changing the control parameter ν. In Figs. 8(d)–8(f) the time series of A_2 are plotted for $\nu=0.017\ 46$, away from the crisis point, still in the periodic regime of A_2 [see Fig. 1(a)]. For $\sigma=0.002\ 72$ the dynamics is still confined to the basin of attraction of A_2 [Fig. 8(d)], but resembles the noise-free chaotic time series of Fig. 8(a). By increasing the noise level to $\sigma=0.002\ 88$ we see an attractor hopping from A_2 to A_1 after a long transient [Fig. 8(e)]. With larger noise ($\sigma=0.003\ 04$) the transient is shortened [Fig. 8(f)]. Evidently, the duration of transients is also related to the initial conditions, and a precise determination of the critical noise level for attractor hopping to occur must rely on the average among several initial conditions and long time series.[30] The important conclusion here is that the presence of noise in an Alfvén system can lead to an attractor destruction, with the dynamics on their basins becoming transient, just as occurs after a boundary crisis. This type of noise-induced crisis was extensively studied by Sommerer et al.[31]

V. NOISE-INDUCED INTERMITTENCY AND ATTRACTOR MERGING

In the previous section it was shown that for $\nu=0.017\ 46$ a small amount of noise ($\sigma=0.00544$) in Eqs. (2)–(4) can drive the solutions from attractors A_2 and A_4 to A_1. In order to induce an "escape" from attractor A_1 it is necessary to increase σ, since the basin of attractor A_1 is much wider than the basins of A_2 and A_4. For large enough σ, trajectories on the basin of A_1 can cross the basin bound-

ary, moving toward a different attractor. The noise will, then, trigger attractor hopping until the trajectory eventually is re-injected into the basin of A_1. This process repeats intermittently, generating the noise-induced (or extrinsic) intermittency.[27]

Figure 9 depicts a time-2π time series at $\nu=0.017\ 46$ for $\sigma=0.064$. Most of the time the value of the b_z component of the Alfvén magnetic field oscillates around 0.78, in the vicinity of A_1. There are several intermittent "bursts" to lower values of b_z, indicating an excursion of the trajectory through a different region of the (b_y, b_z) phase plane. The triangles and squares indicate when the trajectory is in the vicinity of attractors A_2 and A_4, respectively. We consider a vicinity defined as the disk with radius equal to σ around the fixed points of the periodic attractors in the Poincaré map. Figure 9(b) is an enlargement of a part of Fig. 9(a) (indicated by the bar) showing attractor hopping. Note that in every burst there are some points that are not in the vicinity of either A_2 or A_4. Those points represent the time the trajectory spends around the complex basin boundary region, before converging to the vicinity of an attractor. This dynamics is shown in the Poincaré map in Fig. 10, where we plot the noisy basins of attraction and the Poincaré points corresponding to the time series of Fig. 9. Most points concentrate in a stretched region around A_1 and the scattered points rep-
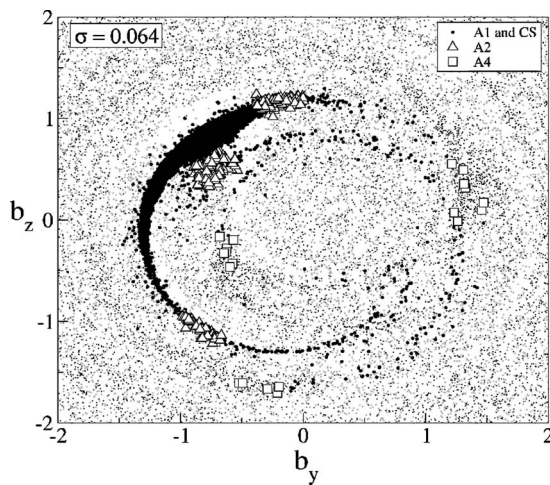
FIG. 10. Basins of attraction and Poincaré points of the intermittent noisy trajectory of Fig. 9 at $\nu = 0.017\,46$. The trajectory spends most of the time in the basin of A_1, and hops among A_1, A_2, and A_4 through the chaotic saddle in the basin boundary. The noise level is $\sigma = 0.064$.

resent the intermittent bursts. From Fig. 10 it can be seen that noise is responsible for merging the three attractors, generating a much wider attractor.

A comparison between Fig. 10 and Fig. 3 reveals that in each burst the trajectory visits the neighborhood of the chaotic saddle. This occurs because, although the chaotic saddle is not attracting, it possesses a *stable manifold*, which is a fractal set in the phase plane whose points display trajectories that converge to the chaotic saddle.[32] Numerical uncertainties and/or extrinsic noise will always drive trajectories away from the stable manifold, thus, orbits close to the stable manifold will first approach the chaotic saddle, then display chaotic motion for a finite time, before moving toward some attractor. In the present case, the stable manifold is the boundary between the basins of attraction shown in Fig. 2. When noise drives a trajectory toward the basin boundary, the boundary leads it to the vicinity of the chaotic saddle. That is the reason why the black points in Fig. 10 are not spread throughout the whole phase plane.

The noise-induced Alfvén intermittency displays the following sequence of states: $A_i \rightarrow$ chaotic saddle $\rightarrow A_i$ $\rightarrow$ chaotic saddle $\rightarrow A_i \rightarrow$ chaotic saddle $\cdots$, where i is either 1, 2, or 4 and represents the time the trajectories are in the vicinity of the noisy periodic attractors.

VI. CONCLUSION

We have studied the dynamics of Alfvén waves in a multistable regime of the derivative nonlinear Schrödinger equation in the presence of noise. For low level noise, attractor hopping occurs until the wave settles to an attractor with a wide basin of attraction. In this case, the effect of noise is similar to an attractor destruction due to boundary crisis, with the generation of transient motion in the vicinity of the destroyed attractors (extrinsic transient). For a higher level of noise, intermittent attractor hopping sets in (extrinsic intermittency), and trajectories have access to a wide region of the phase space, which includes three attractors and a chaotic

saddle embedded in the basin boundary. In both cases (extrinsic transient and extrinsic intermittency), the noise is responsible for "hiding" the attractors of the noise-free system, as previously pointed by Kraut *et al.*[30] Since noise sources are always present in space and laboratory plasmas, it is possible that the transient and intermittent phenomena observed in real data are in fact a signature of multistable regimes in the presence of noise.

Finally, we stress that knowledge of the different attractors and chaotic saddles of a system opens the possibility of using control techniques to suppress the random bursts of amplitude jumps in the intermittent regime, as recently shown by Meucci *et al.*[33] for a model and in a real experiment with a CO_2 laser. Such technology may be of interest for turbulence control in confined plasmas.

[1] P. Y. Cheung and A. Y. Wong, Phys. Rev. Lett. **59**, 551 (1987).
[2] F. Greiner, T. Klinger, H. Klostermann, and A. Piel, Phys. Rev. Lett. **70**, 3071 (1993).
[3] T. E. Sheridam, Phys. Plasmas **12**, 080701 (2005).
[4] K. F. He, Phys. Rev. Lett. **80**, 696 (1998).
[5] K. F. He and A. C.-L. Chian, Nonlinear Processes Geophys. **12**, 13 (2005).
[6] A. C.-L. Chian, F. A. Borotto, and E. L. Rempel, Int. J. Bifurcation Chaos Appl. Sci. Eng. **12**, 1653 (2002).
[7] S. J. Hahn and K. H. Pae, Phys. Plasmas **10**, 314 (2003).
[8] J. T. Seo, K. H. Pae, and S. J. Hahn, Phys. Plasmas **11**, 5364 (2004).
[9] J. C. P. Coninck, S. R. Lopes, and R. L. Viana, Phys. Rev. E **70**, 056403 (2004).
[10] C. S. Chern and L. I, Phys. Rev. A **43**, 1994 (1991).
[11] H. Y. Sun, L. X. Ma, and L. Wang, Phys. Rev. E **51**, 3475 (1995).
[12] P. J. Cargill, Adv. Space Res. **26**, 1759 (2000).
[13] L. Del Zanna and M. Velli, Adv. Space Res. **30**, 471 (2002).
[14] K. Stasiewicz, P. Bellan, C. Chaston, C. Kletzing, R. Lysak, J. Maggs, J. O. Pokhotelov, C. Seyler, P. Shukla, L. Stenflo, L. A. Streltsov, and J. E. Wahlund, Space Sci. Rev. **92**, 423 (2000).
[15] S. Poedts and W. Kerner, J. Plasma Phys. **47**, 139 (1992).
[16] A. G. Elfimov, D. W. Faulconer, K. H. Finken, R. M. O. Galvao, A. A. Ivanov, R. Koch, S. Y. Medvedev, and R. Weynants, Nucl. Fusion **44**, S83 (2004).
[17] C. Grebogi, R. Ott, and J. A. Yorke, Physica D **7**, 181 (1983).
[18] C. Grebogi, E. Ott, F. Romeiras, and J. A. Yorke, Phys. Rev. A **36**, 5365 (1987).
[19] E. L. Rempel and A. C.-L. Chian, Phys. Rev. E **71**, 016203 (2005).
[20] A. C.-L. Chian, F. A. Borotto, E. L. Rempel, and C. Rogers, Chaos, Solitons Fractals **24**, 869 (2005).
[21] T. Hada, C. F. Kennel, B. Buti, and E. Mjolhus, Phys. Fluids B **2**, 2581 (1990).
[22] G.-H. Hsu, E. Ott, and C. Grebogi, Phys. Lett. A **127**, 199 (1988).
[23] E. L. Rempel and A. C.-L. Chian, Int. J. Bifurcation Chaos Appl. Sci. Eng. **14**, 4009 (2004).
[24] A. C.-L. Chian, F. A. Borotto, and W. D. Gonzalez, Astrophys. J. **505**, 993 (1998).
[25] E. Marsch and C.-Y. Tu, J. Geophys. Res. **95**, 8211 (1990).
[26] R. Bruno and V. Carbone, Living Rev. Solar Phys., 2005, Vol. 2, p. 4; online article, http://www.livingreviews.org/lrsp-2005-4.
[27] E. G. Gwinn and R. M. Westervelt, Phys. Rev. Lett. **54**, 1613 (1985).
[28] E. G. Gwinn and R. M. Westervelt, Phys. Rev. A **33**, 4143 (1986).
[29] F. T. Arecchi and F. Lisi, Phys. Rev. Lett. **49**, 94 (1982).
[30] S. Kraut, U. Feudel, and C. Grebogi, Phys. Rev. E **59**, 5253 (1999).
[31] J. C. Sommerer, E. Ott, and C. Grebogi, Phys. Rev. A **43**, 1754 (1991).
[32] H. E. Nusse and J. A. Yorke, Physica D **36**, 137 (1989).
[33] R. Meucci, E. Allaria, F. Salvadori, and F. T. Arecchi, Phys. Rev. Lett. **95**, 184101 (2005).